International Journal of Environmental Science and Technology (2026) 23:276
https://doi.org/10.1007/s13762-026-07063-x

ORIGINAL PAPER

Temporal evolution of polycyclic aromatic hydrocarbons in sediments of the Hooghly river, West Bengal, India

M. Toscanesi[1] · M. Arienzo[2] · L. Ferrara[1] · P. Mondal[3] · M. P. Jonathan[4] · S. K. Sarkar[3] · C. Donadio[2] · M. Trifuoggi[1]

Received: 14 July 2025 / Revised: 30 December 2025 / Accepted: 2 January 2026 / Published online: 3 February 2026

Abstract

The study evaluated the effect of monsoons on the levels of polycyclic aromatic hydrocarbons in the Hooghly River estuary sediments over 2018–2021. It was observed a cyclical enrichment of organic material, carbonate deposits, and clay over the post-monsoon and impoverishment over the monsoon because of the heavy rains and flood events. The mean total level of polycyclic aromatic hydrocarbons was 1682 ng/g with a wide range of variability depending on the season, 125–6518 ng/g, higher than previous assays and lower than a contemporary survey. Also, there was a marked predominance of the polycyclic aromatic hydrocarbon heavy pool, ~ 83%, with fluoranthene and pyrene making more than 40% of the total hydrocarbons loads and with a large variability of the composition with the monsoon. Concerning the numerical sediment quality guidelines, the mean individual compound levels, and ∑PAHs, do not surpass effect range low, effect range median, and apparent effects threshold limits and keep fairly below thresholds with no evidence of detrimental biological consequences. Temporal trends of polycyclic aromatic hydrocarbons split over two periods after the 2019 monsoon, with a sudden drop in hydrocarbon levels from two times for naphthalene, acenaphthylene, pyrene, benzo(a)anthracene, chrysene, to 6–7 times for phenanthrene, benzo(b)fluoranthene, benzo(a)pyrene, and indeno[1,2,3-cd]pyrene, with an overall decrease of ∑PAHs of threefold from 2948 to 959 ng/g. Monsoon seems to play as a sort of natural attenuation effect, slowing down river decline.

Keywords Hooghly river · Ecological risk assessment · Monsoon seasons · Polycyclic aromatic hydrocarbons · Sediment pollution · Sundarban mangrove wetland

Abbreviations

PAHs	Polycyclic aromatic hydrocarbons
HR	Hooghly river
HRE	Hooghly river estuary
SMW	Sundarbans mangrove Wetland
LPAHs	Light-molecular weight PAHs
HPAHs	High-molecular weight PAHs
FA	Freshwater area
BA	Brackish area
EA	Estuary area
OC	Organic carbon
$CaCO_3$	Calcium carbonate
NAP	Naphthalene
ACY	Acenaphthylene
ACE	Acenaphtene
FLR	Fluorene
PHE	Phenanthrene
ANT	Anthracene
FLT	Fluoranthene
PYR	Pyrene
BaA	Benzo(a)Anthracene
CHR	Chrysene
BbF	Benzo(b)Fluoranthene
BkF	Benzo(k)Fluoranthene

Editorial responsibility: Samareh Mirkia.

✉ M. Arienzo
michele.arienzo@unina.it

[1] Dipartimento di Scienze Chimiche, Università Degli Studi di Napoli Federico II, Complesso Universitario di Monte Sant'Angelo, Via Cintia 26, 80126 Naples, Italy

[2] Dipartimento Di Scienze Della Terra, Dell'Ambiente e Delle Risorse, Università Degli Studi di Napoli Federico II, Complesso Universitario di Monte Sant'Angelo, Via Cintia 26, 80126 Naples, Italy

[3] Department of Marine Science, University of Calcutta, 35 Ballygunge Circular Road, Calcutta 700019, India

[4] Centro Interdisciplinario de Investigaciones y Estudios Sobre Medio Ambiente y Desarrollo, Instituto Politécnico Nacional, Calle 30 de Junio de 1520, Barrio la Laguna Ticomán, C.P. 07340 Del. Gustavo A. Madero, Ciudad de Mexico, Mexico

BaP	Benzo(a)Pyrene
DhA	Dibenz(ah)Anthracene
IPY	Indeno[1,2,3-cd]Pyrene
BgP	Benzo(ghi)Perylene
Pre-M	Pre-monsoon
M	Monsoon
Post M	Post monsoon
ERM	Effect range-median
ERL	Effect range low
AET	Apparent effects threshold
SQGs	Standard quality guidelines
CM	Correlation matrix
PCA	Principal component analysis
HCA	Hierarchical cluster analysis
MPCs	Maximum permissible concentrations
RQ	Risk quotient

Introduction

Numerous estuaries create extremely dynamic coastal ecosystems and exhibit hydrographic instabilities over a wide range of spatiotemporal scales (McLusky and Elliott 2004). Besides the complexity brought by freshwater and marine inflows (Wetz and Yoskowitz 2013), the quality of estuary habitats is affected by many natural and anthropic stressors from home, industrial, and agricultural activities, as well as reclamation of estuary ecosystems for urban and industrial developments (Cardoso et al. 2008). The growing frequency of extreme flood and drought events caused by global climate change impacts biodiversity and functioning of estuarine ecosystems (Barroso et al. 2018). Episodic floods releasing consistent quantities of hydraulic energy can have an impact on estuary eco-hydrography and cause notable fluctuations in the abundance and biota community composition, influencing the dynamics of flow, salinity, nutrient distribution, and sediment properties (Wetz and Yoskowitz 2013).

Floods also alter benthopelagic habitats by increasing the deposition of fine sediments and organic litter of terrigenous origin (Norkko et al. 2002; Cardoso et al. 2008). How the estuarine biota reacts to habitat disturbances brought on by episodic floods depends on the flood's intensity, magnitude, and duration in relation to the life cycle of its inhabitants as well as the eco-morphological and bathymetrical characteristics of the estuaries (Currie and Small 2005; Dittmann et al. 2015).

Due to the combined effects of the southwest monsoon and two low-pressure systems that developed in the Bay of Bengal, several Indian states, including West Bengal, experienced an exceptionally high monsoon spell from June 1st to August 19th, 2018. The most notable period occurred from August 8–19th (Vineetha et al. 2020). During this period many devastating episodic floods caused extensive environmental devastation, infrastructural damage, and human casualties because of the state's unrelenting rains, which resulted in massive surface runoff (http://cwc.gov.in/main/downloads/KeralaFloodReport/ Rev-1) of water mixed with sediments.

The Hooghly River, HR, forms a sizable estuary in West Bengal and is the Ganges' westernmost tributary. The discharge of contaminated waters into the HR, which has a catchment area of 6104 km2, is caused by a number of cities built along its banks, as well as chemical, paper, and pulp businesses, tanneries, thermal power stations, and textile and jute mills (Fig. 1). (Mondal et al. 2018; Sadhuram et al. 2005). The Sundarbans Mangrove Wetland (SMW), a UNESCO World Heritage site and a highly fragile ecosystem, is part of the Hooghly River Estuary (HRE), which is formed by the alluvial deposits of the Ganga and Brahmaputra Rivers (Mondal et al. 2018).

One of the biggest tropical estuaries on India's east coast, HRE is eutrophic and well-known for its rich aquatic benthos and plankton variety, as well as its commercially viable fishing (Menon et al. 2000; Rajaneesh et al. 2015). Due to rising urbanization, the estuarine ecology has become extremely vulnerable, with the majority of its biota in danger of going extinct. The Hooghly River Estuary, HRE, is regarded as a "monsoonal estuary" due to the impact of the rainy Indian Summer Monsoon (June–September) (Shetye 2011). The extreme climatic gradients typical of such environment drive physico-chemical weathering, detritus erosion, and intensive biogeochemical activities (Garzanti et al. 2008, 2009), with freshwater inflows surpassing tidal flows (Rogers et al. 2013).

The Brahmaputra provides 700×10^6 tons of sediment to the delta each year, whereas the Ganges River contributes 500×10^6 tons (Zuloaga et al. 2013). The sediment load in the river mouth is rather constant. As a result, the high runoff during the monsoon and the eight-month low runoff during the dry season cause significant temporal fluctuations in salinity, water flow, and pollution burdens. The poor water quality index of the HRE is detrimental to the aquatic biota (Mitra et al. 2017). The chemical makeup of the water is influenced by flows, monsoon seasons, and the amount of silt transported into and deposited in the estuary. PAHs are hydrophobic chemicals with low water solubility and volatility which further reduces with molecular weight increasing (Ferrara et al. 2020). Certain PAHs as phenanthrene, due to their low molecular weight, have a greater vapor pressure and consequently can be found at room temperature as gases or linked with particles (Ravindra et al. 2008a, 2008b). Others, such as the heavier benzo(a)pyrene, are nearly entirely adsorbed onto particles. Natural processes, such as diagenesis, and man-made inputs, can produce PAHs. Human pressure is

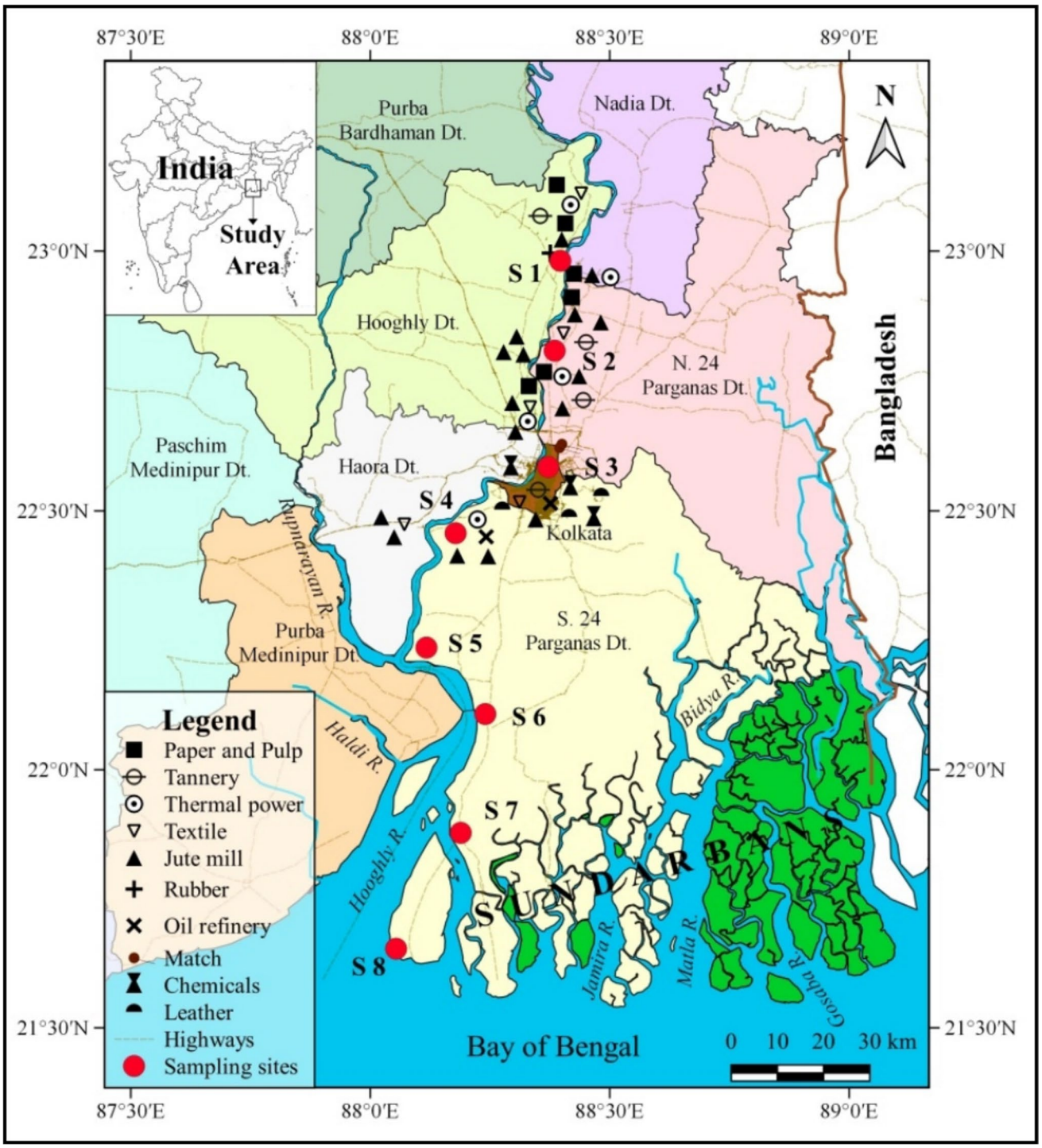

Fig. 1 Location of the main industries, river network, and sampling sites (WGS84 geographic coordinate system)

typically the primary cause of PAH contamination and fall into two primary categories: petrogenic and pyrogenic. Pyrogenic sources include incomplete combustion processes and dry and wet atmospheric fallout, whereas petrogenic sources, mainly include oil spills of crude and refined petroleum products, urban runoff, household and industrial wastewater discharges, ship traffic, and garbage discharges (Hassan et al. 2015). The estuarine area functions as a sink of PAHs. According to Boitsov et al. (2009), the deposition of PAHs in sediments can happen when they are attached to the particulate phase in the atmosphere, settle on water surfaces, finally collect in the

sediment phase, enter pore fluids, and adhere to colloids through the pores. Moreover, the drastic changes of water feature due to fresh and saline waters mixing and PAHS scant solubility, make the chemicals aggregate or sorb with suspended material and precipitate, concentrating in sediments via flocculation Zuloaga et al. 2013). The coexistence of pyrolytic, petrogenic, and early diagenesis forms of PAHs makes it difficult to identify their source in sedimentary deposits. Despite being hydrophobic substances, PAHs have a specific water solubility that influences their marine dispersion (Guigue et al. 2017). Additionally, their chemical reactivity (oxidation, photooxidation) may aid in changing the initial dispersion pattern of the emission sources (Butler and Crossley 1981). PAHs can undergo photooxidation in the shallow water column (Mill et al. 1981), be broken down by microbial activity in the sediments (Cerniglia and Heitkamp 1989), and have an impact on sediment accumulation (Smith and Levy 1990) in estuarine environments. PAHs are divided into two categories: light-molecular weight PAHs (LPAHs, which have two or three aromatic rings) and high-molecular weight PAHs (HPAHs, which have four or more rings). They are released as either particulate HPAHs or gaseous LPAHs, depending on their molecular weight (Lee and Vu 2010). PAH contamination in HR and SMW is extremely rare (Dominguez et al. 2010; Zuloaga et al 2013; Balu et al. 2020). A survey of PAHs profiles in estuarine areas allows the creation of better reference data in terms of trends and origin assessment. In rivers, more than 90% PAHs, remain linked to solid phase and do not enter estuary areas (Murphy et al. 1988). Due to their dangerous effects, PAHs are defined by the US EPA priority pollutants (Chen et al. 2013) HPAHs have teratogenic, mutagenic, and carcinogenic effects, and LPAHs PAHs have high and acute toxicity effects (Hassan et al. 2015).

The goal of the current study was to characterize the impact of severe episodic floods and monsoon cycling on the levels of PAHs in HRE and SMW sediments over a long period of time—from 2018 to 2021—that had never been studied before. The study specifically intends to: (1) evaluate the spatial distribution of PAHs throughout the monsoon seasons and compare them with current regulations and prior research; (2) identify potential anthropogenic and natural sources of pollutants; and (3) evaluate the level of ecological risk associated with PAHs in Hooghly River and SMW deposits. Plans for effective pollution control will benefit from the findings.

Study area

HR, from 87°55′01″N to 88°48′04″N of latitude, and 21°29′02″E to 22°09′00″E of longitude (Fig. 1), has a mean depth of about 6 m (Sadhuram et al. 2005; Mitra et al. 2017), spans a basin of 6104 km^2, and is intensively populated (Mondal et al. 2018). HRE is defined by the presence of the SMW delta, which was created by fluvial-marine deposits. Sediments offshore are impacted by large tides, seasonal monsoons, and tropical cyclones that cross the Bay of Bengal (Roger et al. 2013).

Materials and methods

Climatic outline of the study area

The East Asian summer monsoon, which has yearly precipitations concentrated between April and September, affects the climatic characteristics of HRE (Trifuoggi et al. 2022). Monsoons are extremely erratic, causing periodic droughts and floods, as well as rising sea levels and subsequent coastal area flooding, as is typical in the tropics. Many rivers spread their banks, frequently causing nearby communities to flood. Nearly all of India is at high risk of flooding, and during the past few decades, as temperatures have risen, extreme precipitations like flash floods and torrential rains have become more frequent (Parthasarathy et al. 1994). There are three distinct monsoon seasons: the pre-monsoon (Pre-M), which lasts from March to June; the monsoon (M), which lasts from July to October; and the post-monsoon (Post-M), which lasts from November to February. Over 70–80% of the precipitation occurs between July and September, with an average of roughly 1700 mm (Rakshit et al. 2014). High river flows of 3000 ± 1000 m3/s result from this, and during the pre-monsoon, they gradually drop to a minimum of 1000 ± 80 m3/s (Ray et al. 2015). The year-round gravitational attraction of the sun and moon causes the estuary to have semidiurnal tides, which range from a minimum of 1.8 m at neap tide to a maximum of 5.5 m at spring tide. The increased rate of sediment accretion in HRE, which varies between 3.0 and 4.8 mm/yr, is caused by these characteristics (Banerjee et al. 2012).

Sampling procedure

From November 2018 to May 2021, 176 sediment samples were taken at 8 locations along the approximately 175-km river. Four of these sites belong to the so-named freshwater area, FA, Tribeni, S1, Barrackpore, S2, Babughat, S3, Budge Budge, S4, and are susceptible only to flood events; two were farther up the Hooghly River and belong to the brackish area, BA: Nurpur, S5, Diamond Harbour, S6, subjected to flood and tidal events; two were definitely marine: Lot 8, S7, and Gangasagar, S8, belong to the estuary area, EA, and were only subject to storm surges and tides (Fig. 1). The chosen areas exhibit a broad range of salinity, ranging from 7.5 to 22.5 psu for the marine locations to 0.13–0.3 psu for the

freshwater sites (Trifuoggi et al. 2022). Using a Van Veen grab, surface sediment samples from the intertidal zones were taken in triplicate, sealed in bags, and stored at 4 °C in a cooler box with ice packs (Arienzo et al. 2024). The sediments were stored at −20 °C for further examination. Sediments were then gently crushed after being oven-dried to a consistent weight at 40 °C.

Analytical procedure

The laboratory samples were obtained by mechanically quartering the samples after they had been oven-dried for 72 h at 40 °C. Dry sediment samples, $\Phi \leq 2000$ µm, were used to measure pH, organic carbon, OC (%), $CaCO_3$ (%), granulometry, micromorphology, and PAHs (Arienzo et al. 2017, 2024; Ferrara et al. 2020). The determination of the organic carbon was performed as TOC on a fraction of 0.5 g of the ≤ 2000 µm sediment. The specimens were assayed by by a total organic carbon analyzer Skalar (Breda, The Netherlands). The load of carbonate was assayed by the methods of Jackson. For granulometry sediments were quartered, weighed and sieved by ASTM stacked sieves, 2000 to 63 µm with ½ ϕ interval in a Ro-Tap shaker for 15 min. Decantation was used to analyze the mud fraction (< 63 µm), which includes very fine sand, silt, and clay, by the Belloni (1969) methodology. Data were processed by dedicated software (Blott and Pye 2001) and the procedure of Folk and Ward (1957) was used for sediment classification. 16 priority PAHs were tested: naphthalene, NAP, acenaphthylene, ACY, acenaphtene, ACE, fluorene, FLR, phenanthrene, PHE, anthracene, ANT, fluoranthene, FLT, pyrene, PYR, benzo(a) anthracene, BaA, chrysene, CHR, benzo(b)fluoranthene, BbF, benzo(k)fluoranthene, BkF, benzo(a)pyrene, BaP, dibenz(ah)anthracene, DhA, indeno[1,2,3-cd]pyrene, IPY), benzo(ghi)perylene (US EPA, 1977). Eight compounds namely BgP,. BaA, BaP, BbF, BkF, Chry, DBA, and IP are classified as possible or likely human carcinogens, and BaP is considered a standard of toxicity due to its outmost carcinogenicity (IARC 1987). The compounds were analysed by a modified IRSA CNR 25 method (Arienzo et al. 2017) using a longer sonication, three hours, Brason (US), power of 300 W and acetone/n-hexane 1:1 v/v instead of cyclohexane. The PAHs were identified and measured using a gas chromatograph (Shimadzu 2010 Plus, Japan) with a fused silica HP5-MS capillary column (30 m × 0.25 mm i.d.) of 0.25 µm (Agilent Technologies, US) and a mass spectrometer (MS-TQ8030-Shimadzu, Japan). The carrier gas flowed at a rate of 1.0 mL/min and was 99.9% pure helium. The IRSA CNR 25 was slightly altered for the PAH analysis (Arienzo et al. 2017) by substituting acetone/n-hexane 1:1 v/v for cyclohexane and utilizing a Brason (US) ultrasonic disruptor with a power of 300 W in pulser mode for a longer sonication time of three hours.

A gas chromatograph (Shimadzu 2010 Plus, Japan) with a fused silica HP5-MS capillary column (30 m × 0.25 mm i.d.), 0.25 µm (Agilent Technologies, US) connected to a mass spectrometer (MS-TQ8030-Shimadzu, Japan) and a carrier gas helium at 99.9% with a flow of 1.0 mL/min was used for the analysis.

The determined average LOD and LOQ values were 3 and 10 ng/g, respectively. Interlaboratory ring tests were used to evaluate the data's quality. The statistical analysis was carried out using STATISTICA v.5 (StaSoft Inc., Tulsa, OK, USA). Principal component analysis (PCA), the Pearson correlation matrix (CM), skewness and kurtosis statistical tests (Zhang et al. 2009), and hierarchical group analysis (HCA) were the factorial assessments.

Calculation of potential erosion

The method suggested by Mohtar et al. (2015) and Fournier (1960) was applied to calculate the basin's potential sediment erosion through the following equation:

$$\log E = 2.65\left(P^2/P_m\right) + 0.46 \log H^{\circ} Tg\mathrm{Im} - 1.56 \quad (1)$$

where E is the annual sediment production (g/m^2), P is the rainfall of the wettest month (mm), Pm is the average annual rainfall (mm), H^0 is the average elevation (m asl), and Im is the average gradient (°) of the catchment. Rainfall information is from the regional Meteorological Centre Kolkata, (http://imdkolkata.gov.in/).

The data used to apply the Fournier (1960) formula come partly from Mohtar et al. (2015) and references therein, as rainfall and average temperatures, partly from https://mausam.imd.gov.in/kolkata/; https://mausam.imd.gov.in/kolkata/mcdata/srf.pdf. The basin elevations (m asl), area (km2), and average gradient (°) were extracted using the Google Earth Pro online GIS functions. The data used to calculate the basin's annual erosion rate, such as elevation of the rainfall station (m asl), precipitation of the wettest month P and annual mean Pm (mm), maximum and minimum elevations (m asl), basin area (km2), and average slope Im (°), using the Fournier formula (1960) that considers erodible sediment covers, were input into a specially developed Excel spreadsheet. This operation resulted in estimating erosion E, referring to the suspended sediment (t/km2/year), the average basin erosion Es (t/year), and soil erosion Eh (mm/year).

Results and discussion

Physico-chemical features of the sediment

pH, OC%, $CaCO_3$%, and the textural percentage of sand, silt, and clay of the eight sites along the 175 km of the Hooghly River were reported in Table 1. Data were split by monsoon seasons, Pre-M, M, and Post-M, where season's data represent the average for that particular season during the three years between November 2018 and March 2021. The pH value was tendentially neutral in FA, and slightly alkaline in BA and EA, mean of 7.33 and 7.52 respectively, due to the increasing influence of marine waters on the river ones. Moreover, FA and BA show a clear decreasing pH pattern from Pre-M to Post-M and this was particularly evident at S6 where pH drops from 7.72 in Pre-M to 7.52 in M and 7.45 in Post-M, likely due to the washing off of alkaline bases with strong rain events.

The range of OC was 0.25–0.62% and generally very low, fluctuating without any discernible spatial pattern. The organic load tends to decrease with the M season and then recovers over the Post-M and this was particularly evident at S4 when the organic load of the sediments shifted from 0.38% during M to 0.62% during the Post-M season. In addition to extreme environmental conditions sediment enrichment of organic material might be influenced by microbial degradation, tidal effects, and the rate of sediment deposition (Antizar-Ladislao et al. 2015). This indicates a cyclical enrichment of the finest enriched organic material through sedimentation over the Post-M and impoverishment over the M, as extreme weather conditions vary. Sediments from various coastal regions of India, as including Mannar Gulf, (Jonathan and Ram Mohan 2003), Cochin (Sunil Kumar 1996), and Muthupet mangroves (Janaki-Raman et al. 2007), have higher levels of OC than those of the current survey. Monsoon season causes the organic matter load to decrease significantly because of the washout and transport effect of the rainfall. Carbonate deposits, $CaCO_3$, fluctuate between 8.75 and 15.36% and were high all over the river but with a decreasing pattern from FA, 12.01% to EA, 10.73% and this is likely due to a higher fluvial load of $CaCO_3$ in the form of carbonate deposits typical of tropical environment (Carthew et al. 2003). As already observed for OC%, carbonates decrease from Pre-M to M and then recover over

Table 1 Geographical, and mean physical and chemical sediment features of the 8 sampled sites over Pre-M, M, and Post-M of the period 2018–2021

Sampling sites	Latitude N	Longitude E	Period	pH	OC (%)	$CaCO_3$ (%)	Sand (%)	Silt (%)	Clay (%)
S1 (Tribeni)	22°59′25″	88°24′12″	Pre-M	7.25	0.38	13.81	17.87	31.43	50.69
			M	7.25	0.25	10.60	17.93	30.72	51.36
			Post-M	7.29	0.37	12.44	21.40	30.41	48.20
S2 (Barrackpore)	22°45′51″	88°20′40″	Pre-M	7.44	0.36	15.36	14.20	30.48	55.32
			M	7.43	0.38	11.05	22.45	39.95	37.60
			Post-M	7.38	0.48	13.26	13.68	36.11	50.21
S3 (Babughat)	22°49′32″	88°21′39”	Pre-M	7.47	0.53	11.08	19.07	29.89	51.04
			M	7.46	0.42	10.82	16.87	34.30	48.83
			Post-M	7.30	0.54	12.08	15.14	38.25	46.61
S4 (Budge Budge)	22°33′58″	88°11′16″	Pre-M	7.24	0.43	11.88	14.55	28.05	57.40
			M	7.19	0.38	9.91	18.13	36.36	45.52
			Post-M	7.29	0.62	11.81	13.67	35.74	50.59
S5 (Nurpur)	22°12′40″	88°04′16″	Pre-M	7.68	0.37	11.97	7.10	31.95	60.95
			M	7.59	0.35	9.89	7.64	33.06	59.29
			Post-M	7.53	0.43	11.18	7.59	33.56	58.86
S6 (Diamond Harbour)	22°11′13″	88°11′24″	Pre-M	7.72	0.39	12.35	9.23	29.99	60.78
			M	7.52	0.35	9.54	9.89	34.58	55.53
			Post-M	7.45	0.59	11.22	7.79	33.98	58.23
S7 (Lot 8)	22°52′29″	88°10′09″	Pre-M	7.34	0.37	13.86	7.22	26.10	66.69
			M	7.53	0.40	9.16	13.49	32.82	53.69
			Post-M	7.51	0.46	11.47	11.19	34.02	54.80
S8 (Gangasagar)	22°38′24″	88°04′46″	Pre-M	7.28	0.35	11.75	31.19	26.90	41.92
			M	7.61	0.33	8.75	32.50	32.87	34.62
			Post-M	7.47	0.55	9.36	38.06	27.29	34.65

the Post-M season due to increased removal of the terrigenous fraction from continental deposits as a consequence of heavy rains and floods.

Sediment was silty clay and sandy silty clay, Table 1 (Folk and Ward 1957). The range of clay was quite wide, 34.6–66.7%, increasing from 50.1% in FA to 59.7% in EA. When the Hooghly River connects with the Bay of Bengal, site S8, clay load was low, 37.1% due to energy currents and sediment mixing and removal. It was noteworthy to observe a consistent, ~ 30%, seasonal decrease of clay from Pre-M to M, particularly at S2, where clay content recovered significantly, ~ 32%, over the Post-M. By contrast, lime load varied over a narrower range, 29.02–35.5, with peaks of 35.5% at S3. Regardless of clay concentration, sand content declines from FA to BA, from a mean value of 19.07% at S1 to 10.63% at S7. Concerning the season, sand is enriched in correspondence with M, highlighting consistent processes of transport of coarser grains by erosion. The preponderance of finer silt and clay sediments in the estuary region suggests poor hydrodynamic conditions and freshwater influx with fine particles that accumulate in the bottom side when winds and currents reduce intensity. The marine station S8 of Gangasagar behaves quite differently, with a dominance of coarser deposits due to marine influence that hampers the finest fraction deposition.

The variation of the grain size distribution over the monsoon seasons is depicted in Fig. 2, showing that the silt + clay accounts for 80–90% of the total texture. In correspondence with the high energy M season of 2018, silt and clay show discontinuous and reverse trends, with clay dropping to about half of its previous value before rising again in Post-M. This is probably related to the tremendous force of monsoons, that can remove a constant number of the tiniest particles from the HRE bed. The high susceptibility to erosion of the studied area was confirmed by the output of Mohtar et al. (2015) and Fournier (1960) Eq. (1), revealing a potential high load of suspended solids, 289,000 t/km^2/year, which might cause catastrophic floods (Magdaleno et al. 2018).

PAHs levels in sediments

The mean levels, ng/g, of different PAHs, LPAHs, HPAHs, and ∑PAHs over the eight studied locations and from 2018 to 2021 are shown in Table 2. The sediment quality standards for the Mediterranean coast (Ferrara et al. 2020), the ERL, Effect Range-Low, ERM, Effective Range-Median, and AET, Apparent Effects Threshold, which were described by Long et al. (1995) and derived from the method of Kim et al. (1999), were among the numerical sediment quality guidelines (SQGs) with which the data were compared. These comparisons were performed because of the absence of specific sediment background levels and law limits. The mean total level of PAHs over the entire studied period was 1682 ng/g with a wide range of 125 ng/g recorded during the Post-M in November 2020 and 6518 ng/g detected during the Pre-M in June 2019. This range appeared considerably wider than those reported between 2008 (Binelli et al. 2008), 48.6–1098 ng/g, and 2013 (Zuloaga et al. 2013), 0.4–1839 and lower than a more recent monitoring of 2020 (Balu et al. 2020), 4880–20000 ng/g. This seems to indicate that although the data available in the literature on hydrocarbon levels in the study area are very limited, there has been a considerable increase in contaminant levels in about twenty years with great variability depending on the monsoon seasons and the year of sampling. The distribution of PAHs into light, LPAHs (2–3 rings) and heavy, HPAHs (from 4 to 6 rings) shows that the heavy pool is clearly dominant, with a mean of 1392 ng/g, a share of about 83% of the total pool, and roughly four times higher than that of light ones,

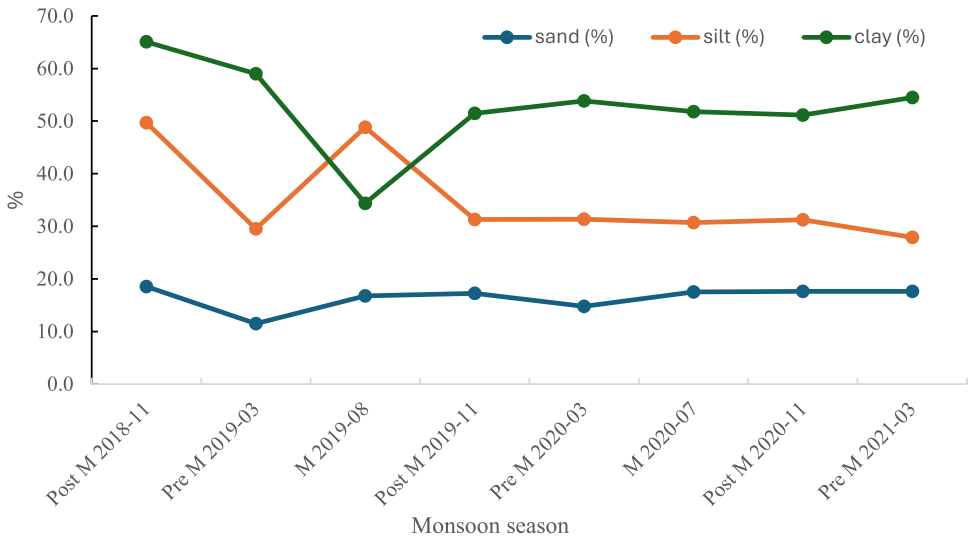

Fig. 2 Variation of granulometric fractions percentages with the monsoon season over 2018–2021

Table 2 Mean concentrations of PAHs in sediments in the period 2018–2021, averaged for all the HRE sampled sites. The concentrations are in ng/g

Time period.	NAP	ACY	ACE	FLR	PHE	ANT	[e]LPAHs	FLT	PYR	BaA
Post M Nov 2018	≤ LOD	3.20	≤ LOD	≤ LOD	92.0	4.59	99.8	97.5	65.7	23.0
Post M Dec 2018	≤ LOD	49.1	≤ LOD	3.59	467	62.2	582	873	520	207
Post M Jan 2018	11.9	71.1	≤ LOD	4.10	924	137	1149	1789	985	236
Post M Feb 2019	16.8	2.58	≤ LOD	6.65	814	287	1127	722	391	55.0
Pre M Mar 2019	≤ LOD	≤ LOD	≤ LOD	≤ LOD	241	≤ LOD	241	197	116	25.9
Pre M Jun 2019	3.80	72.5	0.24	1.38	319	31.4	429	1126	752	267
M Aug 2019	≤ LOD	13.9	≤ LOD	≤ LOD	337	10.4	361	498	299	80.0
Post M Nov 2019	≤ LOD	10.8	≤ LOD	≤ LOD	88.4	4.80	104	147	184	89.6
Mean	4.10	27.9	≤ LOD ≤ LOD	2.00	410	67.2	511	681	414	123
Post M Dec 2019	≤ LOD	5.18	≤ LOD	≤ LOD	56.9	≤ LOD	62.0	128	83.0	36.1
Pre M Mar 2020	9.71	≤ LOD	≤ LOD	≤ LOD	33.2	≤ LOD	42.9	36.8	18.4	5.70
Pre M Jun 2020	≤ LOD	≤ LOD	≤ LOD	≤ LOD	86	10.4	96.8	85.0	50.4	16.9
M Jul 2020	11.0	24.9	≤ LOD	4.58	455	28.1	524	672	102	225
M Aug 2020	≤ LOD	6.33	≤ LOD	1.00	29.2	41.5	78.0	101	67.2	49.4
M Sep 2020	≤ LOD	8.62	≤ LOD	≤ LOD	36.3	52.1	97.0	123	75.1	51.1
M Oct 2020	≤ LOD	15.9	≤ LOD	≤ LOD	52.5	72.9	141.2	148	94.0	65.2
Post M Nov 2020	≤ LOD	3.46	≤ LOD	≤ LOD	7.00	51.8	62.2	41.3	15.6	0.00
Post M Dec 2020	≤ LOD	3.58	≤ LOD	≤ LOD	≤ LOD	46.9	50.4	50.4	24.0	0.00
Post M Jan 2021	≤ LOD	4.35	≤ LOD	1.20	≤ LOD	39.1	44.7	81.0	54.0	2.1
Post M Feb 2021	≤ LOD	7.90	≤ LOD	≤ LOD	≤ LOD	147	155	181	126	10.5
Pre M Mar 2021	≤ LOD	13.2	2.30	7.15	14.2	309	346	892	582	213
Pre M Apr 2021	11.1	28.3	≤ LOD	≤ LOD	33.2	190	263	518	390	123
Pre M May 2021	≤ LOD	21.8	≤ LOD	3.65	72.2	284	381	923	608	247
Mean	2.27	10.25	0.16	1.26	62.60	90.9	*167*	284	164	74.6
Total Mean	*2.92*	*16.7*	*0.12*	*1.51*	*189*	*82.3*	*293*	*429*	*255*	*92.2*
SD	*5.29*	*21.3*	*0.49*	*2.32*	*264*	*99.5*	*259*	*463*	*275*	*93.8*
min	≤ LOD	≤ LOD	≤ LOD	≤ LOD	≤ LOD	≤ LOD	*42.9*	*36.8*	*15.6*	≤ LOD
max	*16.8*	*72.5*	*2.3*	*7.15*	*924*	*309*	*1148*	*1789*	*985*	*267*
[a]ERL	160	16	44	19	240	85	564	600	665	261
[b]ERM	2100	500	640	540	1500	1100	6380	5100	2600	1600
[c]AET	500		150	350	260	300	1560	1000	1000	550
[d]Italian limit	**35**					**45**		**110**		

Time period.	CHR	BbF	BkF	BaP	DhA	IPY	BgP	[f]HPAHs	∑PAHs
Post M Nov 2018	32.3	37.7	22.6	27.5	4.20	27.1	26.2	364	464
Post M Dec 2018	246	351	207	219	52.2	297	259	3231	3813
Post M Jan 2018	259	332	201	235	5.79	320	301	4665	5814
Post M Feb 2019	71.4	88.6	37.9	63.4	9.26	69.3	55.0	1562	2689
Pre M Mar 2019	37.1	50.9	31.7	55.1	3.76	48.8	53.0	619	860
Pre M Jun 2019	475	739	377	419	126	1024	783	6090	6518
M Aug 2019	130	179	93.9	104	22.8	203	156	1766	2127
Post M Nov 2019	118	160	102	96.2	32.9	94.7	171	1196	1300
Mean	171	242	134	152	32.1	260	225	2436	2948
Post M Dec 2019	61.2	71.8	47.1	64.1	2.68	105	92.6	692	754
Pre M Mar 2020	12.8	12.1	5.6	37.2	≤ LOD	14.8	18.8	162	205
Pre M Jun 2020	27.7	31.1	15.1	32.4	≤ LOD	38.3	39.6	337	379
M Jul 2020	264	334	202	235	≤ LOD	449	294	2778	3302
M Aug 2020	44.8	≤ LOD	≤ LOD	≤ LOD	≤ LOD	≤ LOD	≤ LOD	262	340

Table 2 (continued)

Time period.	CHR	BbF	BkF	BaP	DhA	IPY	BgP	[f]HPAHs	∑PAHs
M Sep 2020	37.9	48.8	17.7	≤ LOD	≤ LOD	≤ LOD	≤ LOD	353	451
M Oct 2020	41.6	32.4	29.5	≤ LOD	≤ LOD	31.9	31.1	473	615
Post M Nov 2020	6.07	≤ LOD	≤ LOD	≤ LOD	≤ LOD	≤ LOD	≤ LOD	62.9	125
Post M Dec 2020	5.96	≤ LOD	≤ LOD	≤ LOD	≤ LOD	≤ LOD	≤ LOD	80.4	131
Post M Jan 2021	16.2	≤ LOD	≤ LOD	≤ LOD	≤ LOD	≤ LOD	≤ LOD	153	198
Post M Feb 2021	31.2	≤ LOD	≤ LOD	≤ LOD	310	≤ LOD	≤ LOD	660	815
Pre M Mar 2021	138	≤ LOD	≤ LOD	≤ LOD	≤ LOD	≤ LOD	≤ LOD	1825	2171
Pre M Apr 2021	112	≤ LOD	≤ LOD	≤ LOD	≤ LOD	≤ LOD	≤ LOD	1142	1405
Pre M May 2021	164	79.9	54.5	≤ LOD	≤ LOD	19.9	59.4	2156	2537
Mean	68.8	43.6	26.5	26.3	22.4	47.0	38.3	*795*	*959*
Total Mean	*106*	*116*	*65.7*	*72.2*	*25.9*	*125*	*106*	*1392*	*1682*
SD	*116*	*180*	*97.6*	*110*	*69.6*	*236*	*180*	*1583*	*1814*
min	*5.96*	≤ LOD	≤ LOD	≤ LOD	≤ LOD	≤ LOD	≤ LOD	*62.9*	*125*
max	*475*	*739*	*377*	*419*	*310*	*1024*	*783*	*6090*	*6518*
[a]ERL	384			430				2340	2904
[b]ERM	2800			1600				1.37×10^4	$2.0x10^4$
[c]AET	900			700				4150	5710
[d]Italian limit		**40**		**30**		**70**	**55**		**800**

[a]ERL: Effects range low value.

[b]ERM: effects range medium value.

[c]AET: apparent effects threshold (Kim et al. 1999).

[d]Italian rules, law nr. 219/2010 (Ferrara et al. 2020).

[e]LPAHs: NAP, ACY, ACE, FLR, PHE, ANT

[f]HPAHs: FLT, PYR, BaA, CHR, BbF, BkF, BaP, DhA, IPY, BgP.

293 ng/g. The abundance of 4–6 ringed PAHs reported by Balu et al. (2020), Dominguez et al. (2010), and Sarkar et al. (2012) was consistent with this trend. In our survey FLT and PYR predominate, with a total mean of 429 ng/g and 255 ng/g representing 30.1 and 18.3% of the ∑PAHs.

Our hydrocarbon load seems to be lower than those reported for the Adyar Estuary, 13–31,400 ng/g, the Chitrapuzha River, 5050–33,100 ng/g, (Kumar et al. 2016), and the Mumbai Harbour, 17–134,134 ng/g, (Dhananijay et al. 2012). Additionally, our PAHs data range seems to be substantially wider than those reported in the literature for estuaries in other nations as in Australia in the case of the Brisbane River, 148–3079 ng/g (Duodu et al. 2017); in China in the case of the Chongqing River, 221–3205 ng/g (Lei et al. 2019); in the west coast of Tunisia, 40–655 ng/g (Ameur et al. 2010).

Concerning the numerical sediment quality guidelines (SQGs) the mean individual compound levels as well as the total load, ∑PAHs, do not surpass ERL, ERM, and AET limits and keep fairly below the thresholds with no detrimental biological consequences (Kim et al. 1999; McDonald et al. 2000). However, comparison with current legislation for the Mediterranean marine regions, evidenced a clear surpassing of the limits as of twofold for ∑PAHs, 1682 vs. 800 ng/g, and the majority of PAHs as PYR, three–four-fold the limits, 429 vs. 410 ng/g, and BbF, 116 vs. 40 ng/g. ∑PAHs level appeared outstandingly high, especially in correspondence of the first two years of sampling, Post M Jan 2018, 5814 ng/g, and Pre M Jan 2019, 6518 ng/g surpassing the legal limit of 800 ng/g of seven to eight folds, showing worrying contaminant loads which might deserve action for pollution containment.

Furthermore, the use of SQGs for individual compounds has limitations because complex combinations of PAHs can be present simultaneously in sediments under real-world field settings, making it impossible to rule out their cumulative influence (Binelli et al. 2008). Alkylated and other PAH compounds are not included in consensus guidelines, which are based on parent PAHs. There is no indication of mean total PAHs loads above the threshold effect concentration (TEC) of 290,000 ng/g, the likely effect concentration (PEC) of 1,800,000 ng/g, and the extreme effect concentration (EEC) of 10,000,000 ng/g, as suggested by Swartz (1999). Our data also showed the absence of correlation between OC% and PAHs, $r^2 = 0.35$, and seems to meet the contrasting opinions of the literature. Some authors, Liu et al. (2017), report a positive correlation between OC% and the ∑PAHs relating to the consequent more intricate

pore structure of the organic matter, facilitating easier PAHs absorption. Other authors among which Sarkar et al. (2012, 2016) reported by contrast weak correlation. This means that other factors govern PAHs sorption onto sediments as hydrodynamic conditions, textural composition, sediment deposition rate, PAHs input rate, resuspension and redeposition of sedimentary PAHs, mixing arising from physical or biological processes, and microbial decomposition (Sarkar et al. 2016). The mean relative percentage composition of individual PAHs over the four studied years revealed the net abundance of three PAHs scaling as: FLT > PYR > PHE with 25.9, 15.1, and 11.2%, respectively, once again stressing the abundance of the HPAHs pool, with FLT and PYR representing more than 40% of the total pool of PAHs. This trend was confirmed by the percentage composition of the PAHs (median values expressed in ng/g dry weight), which revealed dominance of 4-ring pool, range of 35.9–84.1%, followed by the 2–3 ring pool, 8.3–49.7%, and the 6-ring pool, range of 3.1–38.1%. These ranges of variation also showed the wide variability of the composition depending on the considered monsoon season.

Temporal variations of PAHs concentration profiles during the 2018–2021 monsoon cycle

To better follow the hydrocarbon pattern changes with monsoons, we depict the monthly concentrations of individual PAHs, and ∑PAHs, in Fig. 3a. From this draw, it appears evident a net variation in the levels of PAHsafter monsoon 2019, when there was a sudden drop in PAHs levels. Cross referencing the patterns of Fig. 3 with the means of the two periods, one from Nov 2018 to Nov 2019, and the other from Dec 2019 to May 2021, Table 2, we observed a consistent decrease of PAHs, from two times for NAP, ACY, PYR, BaA, CHR, to 6–7 times for PHE, BbF, BaP, and IPY, with an overall decrease of ∑PAHs of threefold from 2948 to 959 ng/g.

A moderate discontinuity in this trend was observed in the second period in correspondence of the M Jul 2020, when the mean levels of certain PAHs as BaA, BkF, and especially BgP were much higher than those of the first period, 225 vs. 123 ng/g, 202 vs. 134 ng/g, and 449 vs. 260 ng/g, respectively. This punctual marked variation of the hydrocarbon levels might be related to the already observed cyclical enrichment of finest particles and organic material through sedimentation over the Post-M and impoverishment over the M, as extreme weather conditions vary. The strong meteorological event of the M 2019 likely produced a significant removal of sediments, causing the loss of the finer grains and an immediate change in hydrocarbon levels. After this season, the sediment redeposition processes were not enough to recharge the contaminant loads, which were kept low until Pre-M May 2021. Based on the eight assayed monsoon periods along 2018–2010, Fig. 3b, it was observed a strong seasonal variation of the individual PAHs and a similar pattern of variability, with the most critical seasons being Post-M 2018–11 and Pre-M 2019–03. The data reveal that severe weather conditions, such as those that occur during monsoons, can have a strong impact on hydrocarbon sediment richness, through sediment resuspension. Data also show that the anthropic pressure recharge occurring over the post-monsoon seasons was not enough to bring hydrocarbon levels back to pre-monsoon levels and that heavy rainfall might have a polishing contaminant effect at least in the short term.

Correlation analysis

A Pearson correlation matrix (CM, data not shown) was calculated for the entire set of variables encompassing individual PAHs, pH, OC, $CaCO_3$, sand, and clay for the three main seasonal periods, i.e., Pre-M, M, and Post-M. No evidence of correlation of PAHs with clay, silt, and organic carbon pools was found in the monsoon seasons, indicating that particle sizes and organic material were not responsible for hydrocarbon levels. It is likely that in case of extreme climatic events generated by monsoons, PAHs are moved by storm surges and return to suspension (Arienzo et al. 2019), hampering PHAs sediment accumulation on sediment beds and favouring dispersion. PAHs being highly hydrophobic, enrich in sediment with high TOC load (Dahle et al. 2003). Literature reports significant correlations between total PAHs and OC and this occurs when PAH load is > 2000 ng/g (Simpson et al. 1996). In our study, even though the latter threshold is often surpassed, the low range of OC, 0.25–0.62%, might explain the absence of correlation.

LPAHs, except ACY and PHE, show a scant correlation with ΣPAHs, $r = 0.77$, $p < 0.05$, whereas all the HPAHs pool correlate significantly with ∑PAHs, $0.82 < r < 1.0$, $p < 0.05$. Moreover, while among LPAHs, only the pair FLR-PHE, significantly correlated, $r = 0.74$, in the case of HPAHs all the terms strongly correlate each to other, $r \sim 1.00$, $p < 0.05$, revealing a common source of provenience. Among LPAHs, only ACY is interrelated with the high number of ring terms from BaA to BgP, and PHE with FLT and PYR, $r = 1.00$, $p < 0.5$.

During the Pre-M, only ACY and PHE of the LPAHs pool significantly correlated with every term of HPAHs with r in the range of 0.83–0.99 whereas the terms with more than 4 rings and except BaA appeared strongly and positively interrelated, $p < 0.05$, with r close to 1.0. During the M season, it was observed that the three-term ring ACY, FLR, and PHE appeared interrelated with both LPAHs and HPAHs, as well as a significant increase of the number of heavier compounds correlated, r 0.70–1.00 and $p < 0.05$, revealing different sources of provenience. The data also show a variable

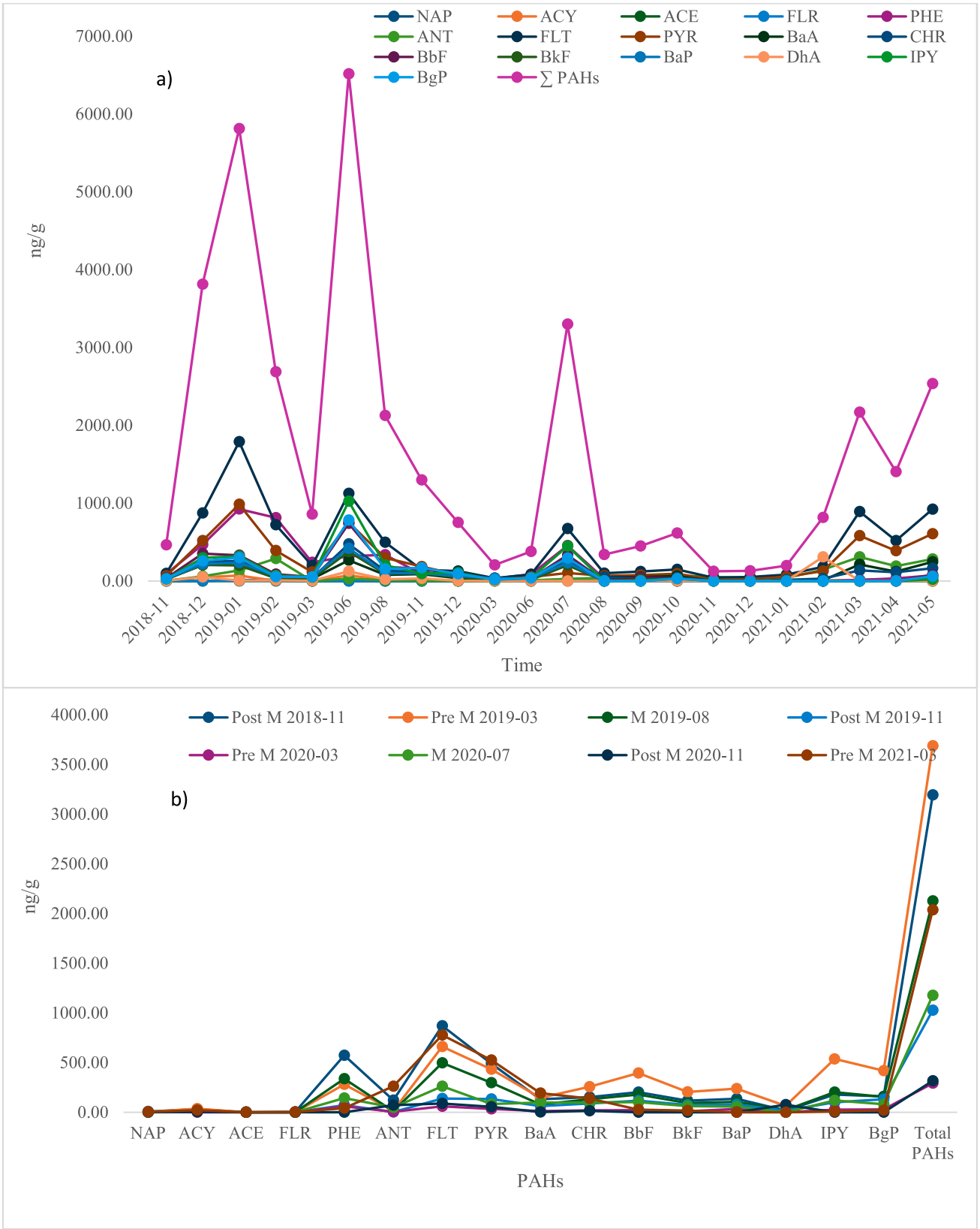

Fig. 3 **a** Monthly and **b** Seasonal levels of PAHs (median values ng/g dry weight) and ∑PAHs

correlation between LMW and HMW, r = 0.63–0.88, significant during Pre-M and M, and not significant during Post-M, suggesting different inputs and deposition processes for LMW and HMW over the seasons.

Factor analysis

Table 3 depicts the results of principal component analysis, PCA, including loading factors, total and cumulative variance from processing as independent variables PAHs, OC, $CaCO_3$, sand, silt, and clay. For Post-M, Pre-M, and M two principal components account for 65.0, 67.05, and 70.8% of the total cumulative variance, respectively. Over the same three seasonal periods, PC1 explains 49.3, 56.2, and 59.4% of the total variance. In Post-M, PC1, except for ACY, a load of 0.90, is not significantly, $p < 0.05$, correlated with LPAHs whereas is highly positively correlated with all sets of single HPAHs. In Pre-M, PC1 groups beside all the individual HPAHs, even ACY, a load of 0.98, and PHE, a load of 0.71, and a practical identical trend was observed over the M, with the addition of the positive load of PHE, 0.85. These data therefore seem to confirm the output generated by the Pearson's correlation, where HPAHs revealed very significant correlation ($p < 0.05$) with $r \geq 0.94$, suggesting meanly a common source of these PAHs, whereas the role of LPAHs increases during the season of strong rain events, when flooding cause sustained addition, erosion, remix and transport of grains.

Hierarchical cluster analysis

Figure. 4 shows the results of the hierarchical cluster analysis (HCA) on the basis of Ward criteria (Lebart et al. 1984). It is possible to distinguish for all the seasons two main clusters, A and B, distinguished at high hierarchical level. In the Post-M, cluster A includes mostly the high molecular weight PAHs and ACY with very short

Table 3 Loading factors, total and cumulative variance of pH, $CaCO_3$, sand, silt, clay, and PAHs for Post-M, Pre-M, and M

	Post-M PC1	PC2	Pre-M PC1	PC2	M PC1	PC2
pH	− 0.15	− 0.33	0.22	− 0.26	− 0.12	− 0.35
% OC	0.18	0.18	− 0.30	0.05	0.17	0.19
% $CACO_3$	0.32	0.00	− 0.30	− 0.08	0.17	0.24
% Sand	0.08	− 0.04	0.65	0.04	− 0.12	0.42
% Silt	0.02	0.23	− 0.60	0.13	0.18	**0.73**
% Clay	− 0.05	− 0.25	0.47	− 0.11	− 0.05	**− 0.83**
NAP	0.19	− 0.55	− 0.53	0.07	0.41	− 0.24
ACY	**0.88**	0.24	0.27	0.05	**0.90**	0.02
ACE	0.40	**− 0.82**	− 0.17	− 0.63		
FLR	0.42	− 0.58	− 0.59	**− 0.82**	**0.86**	− 0.36
PHE	0.51	− 0.58	0.45	0.33	**0.85**	− 0.03
ANT	**0.73**	− 0.62	0.01	**− 0.88**	0.68	− 0.34
FLT	**0.82**	− 0.50	0.13	− 0.27	**0.99**	0.01
PYR	**0.80**	− 0.15	0.42	− 0.29	0.42	0.60
BaA	**0.93**	0.07	0.27	− 0.35	**0.94**	− 0.15
ChR	**0.82**	0.51	− 0.08	− 0.01	**0.99**	− 0.03
BbF	**0.83**	0.51	− 0.07	0.21	**0.99**	0.03
BkF	**0.79**	0.49	− 0.17	0.20	**0.99**	− 0.02
BaP	0.03	0.06	0.11	0.27	**0.97**	− 0.02
DhA	**0.77**	0.47	− 0.12	0.25	0.42	**0.72**
IPY	**0.78**	0.50	− 0.10	0.25	**0.99**	0.01
BgP	**0.96**	− 0.23	0.02	0.23	**0.98**	0.01
TOT PAHs	**0.88**	0.42	− 0.04	0.00	**1.00**	0.03
TOT PD	0.61	− 0.65	− 0.38	0.16	**0.99**	− 0.01
LPAHS	**0.98**	− 0.15	0.08	− 0.35	**0.91**	− 0.08
HPAHS	− 0.15	− 0.33	0.22	0.02	**1.00**	0.05
% total variance	49.30	15.70	56.22	10.82	59.4	11.4
% cumulative	49.3	65.0	56.22	67.05	59.4	70.8

USA, Kentucky USA, Kentucky.

In bold are the significant loads, $p < 0.05$

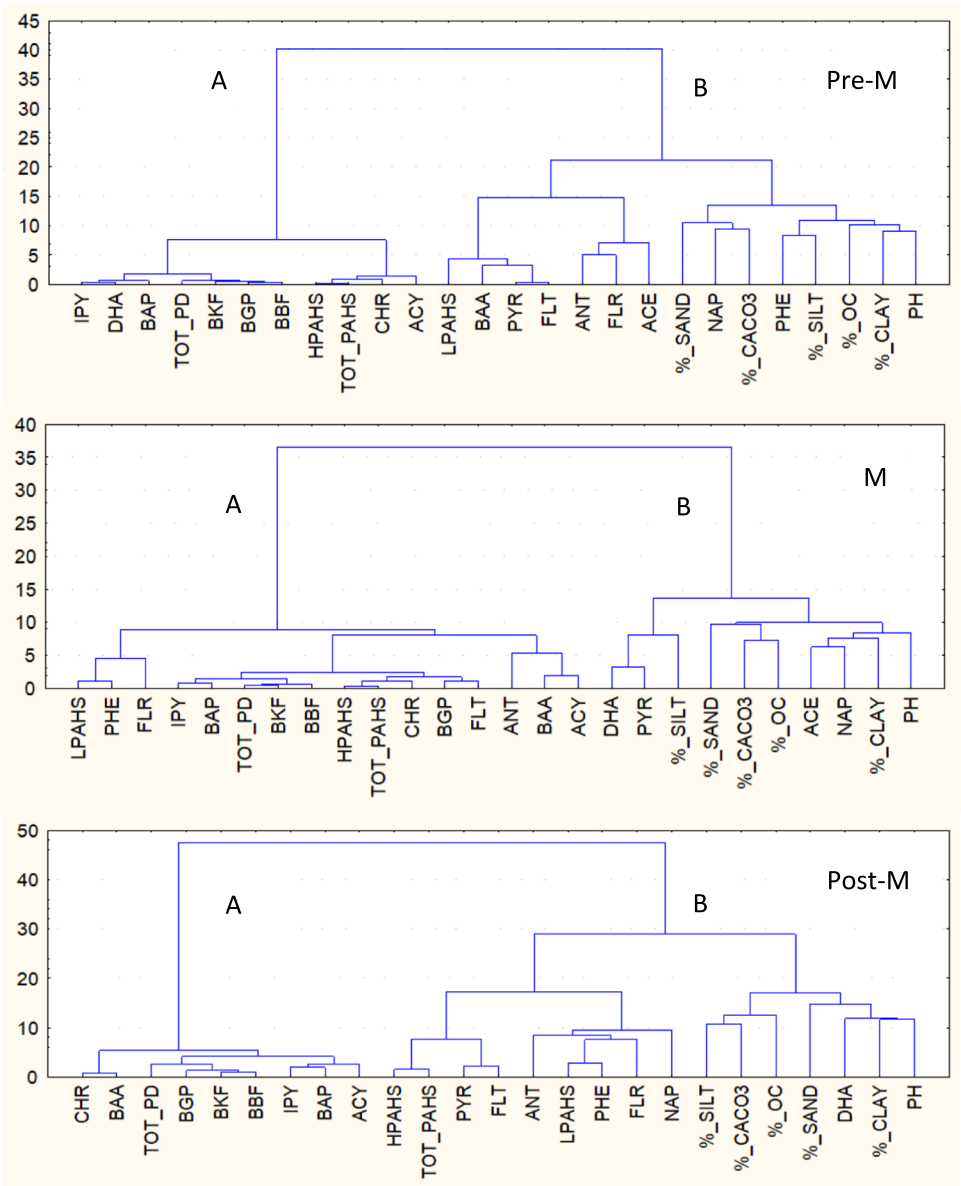

Fig. 4 Hierarchical cluster analysis (HCA). A and B indicate clusters of Pre-M, M, and Post-M seasons

distances. Group B includes two subgroups, one including the low molecular compounds and the other the granulometric features. During the Pre-M, the distribution patterns of the variables under the different groups remain almost unvaried except for one B subgroup, where NAP and PHE associate together with short distances with the physico-chemical sediment parameters. The situation varies with the M season, when the two sub-groups of variables encompassing the light and the heavy hydrocarbon compounds merge together and the distances within each group become narrower. These results sustain and confirm the output of the PCM and PCA which highlighted the consistent association of ACY with heavier terms. In the following Post-M season, the Euclidean distances recover to a certain extent the wideness pattern showed in the Pre-M, due likely to the recovery of the redeposition phenomena during the driest periods.

PAHs sources (pyrogenic vs. petrogenic)

Table 4 reports eleven diagnostic indexes determined in sediment samples that were compared with the reference values, to reveal petrogenic or pyrogenic sources of PAHs. PAHs from petroleum-derived (petrogenic) sources are more concentrated in components with lower molecular weights (two to three-ringed PAHs) while mixtures generated by combustion are primarily four to six-ringed PAHs and thermodynamically more stable and toxic (Adeniji et al. 2018). A consistent number of indices shows that the main source is from combustion and this occurs along all the three

Table 4 Diagnostic ratios determined during monsoon season

Monsoon season	Source												
	PHE/ANT	CHR/BaA	BaP/BgP	FLT/PYR	ANT/ANT + PHE	FLT/FLT + PYR	IPY/IPY + BgP	BaA/BaA + CHR	Ring456/∑PAHs	LPAHs/HPAHs	[b]∑COMB/∑PAHs
Post M 2018	4.68	1.17	0.85	1.77	0.18	0.64	0.53	0.46	0.77	0.31	0.71
Pre M 2019	17.8	1.75	0.57	1.53	0.05	0.60	0.56	0.36	0.91	0.10	0.75
M 2019	32.5	1.63	0.67	1.67	0.03	0.63	0.57	0.38	0.83	0.18	0.72
Post M 2019	30.3	1.42	0.61	1.03	0.03	0.51	0.43	0.41	0.92	0.09	0.80
Pre M 2020	11.5	1.79	1.19	1.77	0.08	0.64	0.48	0.36	0.85	0.28	0.76
M 2020	2.95	0.99	0.72	3.08	0.25	0.76	0.60	0.50	0.82	0.22	0.72
Post M 2020	0.02	4.73		1.61	0.98	0.62		0.17	0.75	0.33	0.51
Pre M 2021	0.15	0.71	0.00	1.48	0.87	0.60	0.25	0.58	0.84	0.19	0.83
Petrogenic	> 15	< 0.4		< 1	< 0.1	< 0.4	< 0.2	< 0.2	< 0.4	> 1	< 1
Pyrogenic	< 10	> 0.9	> 0.6	> 1	> 0.1	≥ 0.5	> 0.5	> 0.35	> 0.5	< 1	~ 1

[a]Ring456: Total 4–6 ring PAHs (mostly originated from combustion); [b]∑COMB (FLT, PYR, BaA, CHR, BbF, BkF, BaP, BgP).In our study, the ratio of LPAHs/HPAHS, 0.09–0.33 was largely below the threshold for pyrogenic source (combustion derived) < 1, dominated by 4-ring or higher molecular weight PAHs

monsoon seasons. An exception to this trend was observed in 2019, when PHE/ANT and ANT/ANT + PHE, highlighted a petrogenic provenience of contamination. The PHE/ANT and ANT/ANT + PHE are considered as the most frequently used indexes to distinguish between combustion and petroleum sources (Yunker et al. 2002). These indices show that over all the monsoon seasons of 2019 the petrogenic input is quite significant, with PHE/ANT in large excess of the threshold of > 15, especially during M, with PHE/ANT of 32.5, and Post M, PHE/ANT of 30.3. Similarly, and over the same temporal periods, ANT/ANT + PHE was < 0.1, a threshold typical of petrogenic input. It is likely that the strength of the cyclones removes crude oil and petroleum products from lands and banks of the Hooghly River. The periodical petrogenic source of PAHs is confirmed by the ∑COMB/∑PAHs index (Yan et al. 2004), which displays a range of values, 0.51–0.83 in agreement with the threshold of < 1 reported by Arienzo et al. (2017).

Due to physical, chemical, and biological variables, the PAH mixture's long persistence after formation—first in the atmosphere, then in marine waters, and ultimately in sediments—further modifies its initial composition. The first significant distinction between low and high molecular weight, or LMW and HMW, occurs in the atmosphere. Compared to HMW, which are less polar, combine with solid particles, and precipitate with dry or wet deposition, LMW are more volatile and typically have a longer residence time in the atmosphere. PAHs are less prone to breakdown once they are absorbed by sediments (Guzzella and Depaolis 1994). PAHs most likely originate from a variety of sources, including urban runoff, vehicle emissions, river discharges, and domestic usage of coal, charcoal, wood, rice husking, and coal power plants (Chatterjee et al. 2007; Dominguez et al. 2010; Balu et al. 2020).

Potential toxicological assessment

Table 5 shows the equivalent toxicity, TEQ, of the PAHs mixtures, calculated in terms of BaP equivalents. BaP belongs to the group 1 carcinogen, and its metabolites possess high mutagenic effect and hamper DNA replication (Obini et al. 2013). The toxicity equivalency factors (TEF) of the individual PAHs in relation to BaP were used to determine TEQ (Nisbet and La Goy 1992; US EPA 1993). The overall BaP Toxicity Equivalent was calculated using the formula (TEQ TEQ=Cix TEFi), where Ci is the concentration of each PAH (ng/g d.w.) and TEFi is its corresponding TEF. Similarly, the mutagenic and carcinogenic equivalency factors in relation to BaP and 2,3,7,8-tetrachlorodibenzo-dioxin were used to calculate the equivalent mutagenicity, MEQ, and equivalent carcinogenicity, CEQ (Ferrara et al. 2020), Table 5. Additionally, PAHscarc/$_2$PAHs, the ratio of

Table 5 TEQ, MEQ, CEQ, and share of carcinogenic PAHs in PAHs (ng/g)

Time	TEQ	MEQ	CEQ	$PAHs_{canc}/\sum PAHs$
Nov 2018	60.4	56.4	0.26	0.21
Dec 2018	594	507	2.46	0.32
Jan 2018	384	522	2.32	0.19
Feb 2019	141	130	0.54	0.15
Mar 2019	91.2	100	0.37	0.26
Jun 2019	1305	1178	5.34	0.26
Aug 2019	278	267	1.24	0.21
Nov 2019	309	228	1.13	0.46
Mean	395	374	1.71	0.26
Dec 2019	105	142	0.57	0.522
Mar 2020	41.4	49.6	0.09	0.244
Jun 2020	38.1	55.2	0.19	0.197
Jul 2020	363	559	2.47	0.328
Aug 2020	6.01	4.82	0.01	0.050
Sep 2020	12.9	19.0	0.22	0.068
Oct 2020	17.7	33.2	0.27	0.073
Nov 2020	0.65	0.11	0.00	0.029
Dec 2020	0.61	0.10	0.00	0.015
Jan 2021	0.90	0.45	0.00	0.051
Feb 2021	1555	91.4	0.64	0.255
Mar 2021	27.3	19.8	0.03	0.058
Apr 2021	16.3	12.0	0.03	0.069
May 2021	46.8	66.5	0.53	0.098
Mean	161	76.6	0.36	0.151
Overall Mean	*245*	*184*	*0.85*	*0.19*
min	*0.61*	*0.1*	*0*	*0.015*
max	*1555*	*1178*	*5.34*	*0.52*

carcinogenic to total PAHs concentration, was computed (US EPA 2008).

Data show a significant difference between the period from November 2018 to November 2019 and from December 2019 to May 2021, with a mean TEQ of 395 ng/g in the former which was twofold that recorded over the second period, 161 ng/g. A peak of 1305 ng/g was observed in June 2019 at the beginning of the monsoon season and 1555 ng/g in February 2021. These mean TEQ values appear to be similar to those reported by (Zuloaga et al. 2013) for the Sundarbans wetland in Bangladesh, 221 ng/g, and for Sundarbans wetland in India, 358 ng/g. Furthermore, the TEQ overall range of 0.61–1555 ng/g was also comparable with that reported for the same areas of 1.3–1,014 ng/g, and 1.3–2,450 ng/g, respectively (Zuloaga et al. 2013). Similarly to TEQ, MEQ appeared significantly higher over 2019 compared to the other assayed periods, 374 vs. 66.5 ng/g, with a mean share of carcinogenic compounds, which was 26% in 2019 and 15% over 2020–2021. The results evidenced how the toxicity of PAHs mixtures varied markedly with the monsoon seasons, with periods of the year where TEQ and MEQ values resulted several 100-fold higher than those of moderately polluted sites (Adenijii et al. 2019a, 2019b).

Ecological risk

Ecosystems are in extremely high danger when PAHs are present in aquatic environments. To measure the risk that a mixture of PAHs poses to the biosphere, an ecosystem risk assessment was implemented by Wu et al. (2011). This technique was improved by Cao et al. (2010) by using the hazardous equivalency factors for the 16 PAHs reported by the USEPA. The risk quotient, RQ, is the ratio of the contaminant concentration, in this case, a PAH to the predicted ideal value, or CQV, for the same contaminant.

Toxic equivalency factors based on negligible concentrations (NCs), Eq. (2), and maximum allowed concentrations (MPCs), Eq. (3), are employed to define the ecological risk of PAHs (Cao et al. 2010; Wu et al. 2011).

Risk quotients were calculated:

$$RQ_{NCs} = C_{PAHs}/C_{QV(NCs)} \quad (2)$$

$$RQ_{MPCs} = C_{PAHs}/C_{QV(MPCs)} \quad (3)$$

where the values of $C_{QV(NCs)}$ and $C_{QV(MPCs)}$ represent the quality levels of the NCs and MPCs of PAHs, respectively (Ferrara et al. 2020). NC is defined as MPC/100, which takes into consideration the synergistic effects of other chemicals (Cao et al. 2010) and MPCs are concentrations above which the risk is unacceptable with negative consequences. The RQ (NCs) and RQ (MPCs) of PAHs (ng/g) in the sediments under study were displayed in Table 6 and were compared with the risk classes for individual PAHs, free, low, moderate, high, and for mix of ΣPAHs. When considering the individual compound, the risk can be considered very high especially for NAP, ACY, FLR, PHE, ANT, PYR, and BaA and BbF, with risk quotients for both NCs and MPCs, exceeding the threshold of high risk of≥ 1. For the same set of PAHs, the risk of the PAHs mix was also very high, being ∑PAHs relative to MPCs significantly higher than the threshold of 800, and this was particularly evident for Post M 2018 and Pre M 2019 when the threshold was surpassed on the average of about 80-fold, respect to a mean excess of about 20-fold for M. This trend seems to indicate that the ecological risk varies with the season being higher over the recharge phase of pollutants, i.e., after the monsoons and lower over the flooding events during the monsoons.

Table 6 Values of PAHs risk quotients relative to negligible concentrations, NCs, and maximum permissible concentrations, MPCs

	Post M 2018	Pre M 2019	M 2019	Post M 2019	Pre M 2020	M 2020	Post M 2020	Pre M 2021	NCs
NAP	5.12	1.34	0.00	0.00	3.47	1.97	0.00	2.63	1.4
ACY	26.2	30.2	11.6	6.64	0.00	11.6	4.02	17.57	1.2
ACE	0.00	0.10	0.00	0.00	0.00	0.00	0.00	0.64	1.2
FLR	2.99	0.58	0.00	0.00	0.00	1.16	0.26	3.00	1.2
PHE	113	55	66	14	12	28	0	8	5.1
ANT	102	13	8.6	2.0	4.3	41	59	218	1.2
FLT	33	25.4	19.2	5.3	2.3	10.0	3.4	29.9	26
PYR	409	362	249	111	29	71	46	439	1.2
BaA	36	40.7	22.2	17.5	3.1	27.1	0.9	54.0	3.6
CHR	1.42	2.39	1.22	0.84	0.19	0.91	0.14	1.29	107
BbF	56	110	49.7	32.3	6.0	28.9	0.0	7.4	3.6
BkF	8.43	16.5	7.45	4.84	0.90	4.33	0.00	1.11	24
BaP	5.05	8.78	3.85	2.97	1.29	2.17	0.00	0.00	27
DhA	0.66	2.40	0.84	0.66	0.00	0.00	2.87	0.00	27
IPY	6.60	19.9	7.52	3.70	0.98	4.45	0.00	0.25	59
BgP	2.14	5.58	2.08	1.76	0.39	1.09	0.00	0.26	75
RQ∑PAHs(NCs)	808	693	449	204	63	233	117	782	
	Post M 2018	Pre M 2019	M 2019	Post M 2019	Pre M 2020	M 2020	Post M 2020	Pre M 2021	MPCs
NAP	512	134	0	0	347	197	0	263	140
ACY	2625	3022	1159	664	0	1162	402	1757	120
ACE	0	10	0	0	0	0	0	64	120
FLR	299	58	0	0	0	116	26	300	120
PHE	11,259	5494	6611	1424	1173	2811	34	781	510
ANT	10,234	1310	865	200	432	4055	5934	21,764	120
FLT	3348	2545	1917	530	234	1004	341	2991	2600
PYR	40,875	36,154	24,885	11,129	2866	7054	4584	43,864	120
BaA	3620	4067	2222	1746	314	2711	87	5395	360
CHR	142	239	122	84	19	91	14	129	10,700
BbF	5620	10,976	4969	3226	601	2886	0	739	3600
BkF	843	1646	745	484	90	433	0	111	2400
BaP	505	878	385	297	129	217	0	0	2700
DhA	66	240	84	66	0	0	287	0	2700
IPY	660	1987	752	370	98	445	0	25	5900
BgP	214	558	208	176	39	109	0	26	7500
RQ∑PAHs(MPCs)	80,823	69,319	44,923	20,394	6342	23,289	11,709	78,210	

Conclusion

The research highlights that the high-energy events occurring during the monsoon seasons along the Hooghly estuary might have, in the short term, a strong impact on the levels of PAHs. Erosion and transportation of a conspicuous mass of terrestrial sediments driven by strong climatic events can significantly decrease the anthropic load and impact of PAHs, through a multitude of processes: desorption from clay and organic matter, resuspension in the water columns and volatilization/photo-oxidation and microbial degradation. Thus, the monsoon seems to act as a sort of natural attenuation effect of the anthropic flows, even if sediment hydrocarbon richness can be extremely high during post- and pre-monsoon, due to the process of recharge of detrital materials.

Comparison with historical reports seems to sustain that the whole estuary is affected by a significant reduction of pollution loads, likely depending on monsoon intensity and duration, and climatic changes. Thus, the monsoon polishing hydrocarbon effect might slow down the decline of the river and its estuary. The findings necessitate additional research to extend the study duration and establish a scientific foundation for the management of hydrocarbon pollution in areas such as the HRE and the adjacent Sundarban Mangrove Wetland. The results of this study can be used in framing policies centered on restorative measures to resuscitate the historically, economically and culturally important distributary of the River Ganges.

Acknowledgement The co-author Priyanka Mondal thanks the Department of Science and Technology (DST) for the fellowship awarded "Innovation in Science Pursuit for Inspired Research (INSPIRE)".

Author contributions Maria Toscanesi: Conceptualization, Methodology, Data curation, Formal analysis, Validation. Michele Arienzo: Writing original draft, Conceptualization, Methodology, review & editing. Luciano Ferrara: Conceptualization, Methodology.Priyanka Mondal: Investigation, Formal analysis, Validation. Jonathan Muthuswamy Ponniah: Investigation, Formal analysis, Validation. Santosh Kumar Sarkar: Investigation, Formal analysis, Validation. Marco Trifuoggi: Conceptualization, Methodology, Investigation.

Funding Open access funding provided by Università degli Studi di Napoli Federico II within the CRUI-CARE Agreement. The study was founded by the Department of Science and Technology (DST), New Delhi, India [sanction no.: DST/INSPIRE Fellowship/2014/IF140943] under a project named "Distribution and possible sources of trace metals and PAHs in sediments along the Hooghly Estuary and Sundarban Mangrove Wetland, India and their ecotoxicological significance.

Data availability The datasets generated during and/or analysed during the current study are available from the corresponding author on reasonable request.

Declarations

Conflict of interest The authors declare that they have no conflict of interest.

Consent to participate Not applicable.

Consent for publication We do give our consent to publish our data.

Ethical approval Not applicable.

References

Adeniji AO, Okoh OO, Okoh AI (2019a) Distribution pattern and health risk assessment of polycyclic aromatic hydrocarbons in the water and sediment of Algoa Bay, South Africa. Environ Geochem Health 41:1303–1320

Adeniji AO, Okoh OO, Okoh AI (2019b) Levels of polycyclic aromatic hydrocarbons in the water and sediment of buffalo river estuary, South Africa and their health risk assessment. Mar Pollut Bull 84:418–423

Ameur WB, Trabelsi S, Driss MR (2010) Polycyclic aromatic hydrocarbons in superficial sediments from Ghar El Melh Lagoon, Tunisia. Bull Environ Contam Toxicol 85:184–189

Antizar-Ladislao B, Bhattacharya BD, Chaudhuri SR, Sarkar SK (2015) Impact of silver nanoparticles on benthic prokaryotes in heavy metal-contaminated estuarine sediments in a tropical environment. Mar Pollut Bull 99:104–111. https://doi.org/10.1016/j.marpolbul.2015.07.051

Arienzo M, Donadio C, Mangoni O, Bolinesi F, Stanislao C, Trifuoggi M, Toscanesi M, Di Natale G, Ferrara L (2017) Characterization and source apportionment of polycyclic aromatic hydrocarbons (PAHs) in the sediments of gulf of Pozzuoli (Campania, Italy). Mar Pollut Bull 124:480–487. https://doi.org/10.1016/j.marpolbul.2017.07.006

Arienzo M, Toscanesi M, Trifuoggi M, Ferrara L, Stanislao C, Donadio C, Villari G, De Vico G, Carella F (2019) Contaminants bioaccumulation and pathological assessment in *Mytilus galloprovincialis* in coastal waters facing the brownfield site of Bagnoli, Italy. Mar Pollut Bull 140:341–352

Arienzo M, Toscanesi M, Ponniah JM, Ferrara L, Donadio C, Napolitano G, Mondal M, Sarkar SK, Trifuoggi M (2024) First results of a campaign of the measurement of polycyclic aromatic hydrocarbons in the sediments of the Hooghly river, West Bengal, India. J Mar Sci Eng 12:666. https://doi.org/10.3390/jmse12040666

Balu S, Bhunia S, Gachhui R, Mukherjee J (2020) Assessment of polycyclic aromatic hydrocarbon contamination in the Sundarbans, the world's largest tidal mangrove forest and indigenous microbial mixed biofilm-based removal of the contaminants. Environ Pollut 266:115270

Banerjee K, Senthilkumar B, Purvaja R, Ramesh R (2012) Sedimentation and trace metal distribution in selected locations of Sundarbans mangroves and Hooghly estuary, northeast coast of India. Environ Geochem Health 34:27–42

Barroso H, Tavares T, Soares M, Garcia T, Rozendo B, Simone ACV, Patrícia BV, Melo PT, Tasso F, Pereira FJ, Schettini C, Santaella S (2018) Intra-annual variability of phytoplankton biomass and nutrients in a tropical estuary during a severe drought. Estuar Coast Shelf Sci 213:283–293

Belloni S (1969) Una tabella universale per eseguire granulometrie col metodo della sedimentazione unica o col metodo del densimetro di Casagrande modificato. Geol Tecn 16:1281–1289

Binelli A, Sarkar SK, Chatterjee M, Riva C, Parolini M, Bhattacharya B, Bhattacharya AK, Satpathy KK (2008) A comparison of sediment quality guidelines for toxicity assessment in the Sunderban Wetlands (Bay of Bengal, India). Chemosphere 73:1129–1137

Blott SJ, Pye K (2001) GRADISTAT: a grain size distribution and statistics package for the analysis of unconsolidated sediments.

Earth Surf Process Landf 26:1237–1248. https://doi.org/10.1002/esp.261
Boitsov S, Jensen HKB, Klungsøyr J (2009) Natural background and anthropogenic inputs of polycyclic aromatic hydrocarbons (PAH) in sediments of south-western Barents sea. Mar Environ Res 68:236–245. https://doi.org/10.1016/j.marenvres.2009.06.013
Butler JD, Crossley F (1981) Reactivity of polycyclic aromatic hydrocarbons adsorbed on soot particles. Atmos Environ 15:91–94
Cao Z, Liu J, Li YLY, Ma M, Xu J, Han S (2010) Distribution and ecosystem risk assessment of polycyclic aromatic hydrocarbons in the Luan river. China Ecotoxicol 19:827–837
Cardoso PG, Raffaelli D, Lillebø AI, Verdelhos T, Pardal MA (2008) The impact of extreme flooding events and anthropogenic stressors on the macrobenthic communities'dynamics. Estuar Coast Shelf Sci 76:553–565
Carthew KD, Taylor MP, Drysdale RN (2003) Are current models of tufa sedimentary environments applicable to tropical systems? A case study from the Gregory River. Sedim Geol 162:199–218. https://doi.org/10.1016/S0037-0738(03)00151-9
Cerniglia CE, Heitkamp MA (1989). In: Vanarasi U (ed) In microbial degradation of PAH in the aquatic environment. CRC Press, Boca Raton, pp 41–68
Chatterjee M, Silva Filho EV, Sarkar SK, Sella SM, Bhattacharya A, Satpathy KK (2007) Distribution and possible source of trace elements in the sediment cores of a tropical macrotidal estuary and their ecotoxicological significance. Environ Int 33:346–356. https://doi.org/10.1016/j.envint.2006.11.013
Chen CF, Chen CW, Dong CD, Kao CM (2013) Assessment of toxicity of polycyclic aromatic hydrocarbons in sediments of Kaohsiung Harbor, Taiwan. Sci Total Environ 463:1174–1181
Currie DR, Small KJ (2005) Macrobenthic community responses to long-term environmental change in an east Australian sub-tropical estuary. Estuar Coast Shelf Sci 63:315–331
Dahle S, Savinov VM, Matishov GG, Evenset A, Næs K (2003) Polycyclic aromatic hydrocarbons (PAHs) in bottom sediments of the Kara Sea shelf, Gulf of Ob and Yenisei Bay. Sci Total Environ 306:57–71
Dhananjayan V, Muralidharan S, Peter VR (2012) Occurrence and distribution of polycyclic aromatic hydrocarbons in water and sediment collected along the Harbour Line Mumbai, India. Int J Oceanogr. https://doi.org/10.1155/2012/403615
Dittmann S, Baring R, Baggalley S, Cantin A, Earl J, Gannon R, Keuning J, Mayo A, Navong N, Nelson M, Noble W (2015) Drought and flood effects on microbenthic communities in the estuary of Australia's largest river system. Estuar Coast Shelf Sci 165:36–51
Dominguez C, Sarkar SK, Bhattacharya A, Chatterjee M, Bhattacharya BD, Jover E, Albaiges J, Bayona JM, Alam MA, Satpathy KK (2010) Quantification and source identification of polycyclic aromatic hydrocarbons in core sediments from Sundarbans Mangrove Wetland. Arch Environ Contam Toxicol 59:49–61. https://doi.org/10.1007/s00244-009-9444-2
Duodu GO, Ogogo KN, Mummullage S, Harden F, Goonetilleke A, Ayoko GA (2017) Source apportionment and risk assessment of PAHs in Brisbane River sediment, Australia. Ecol Indic 73:784–799
Ferrara L, Trifuoggi M, Toscanesi M, Donadio C, Barra D (2020) Source identification and eco-risk assessment of polycyclic aromatic hydrocarbons in the sediments of seawaters facing the former steel plant ILVA, Naples, Italy. Reg Stud Mar Sci 35:101097
Folk RL, Ward WC (1957) Brazos river bar: a study in the significance of grain size parameters. J Sediment Petrol 27:3–26. https://doi.org/10.1306/74D70646-2B21-11D7-8648000102C1865D
Fournier F (1960) Climat et ´erosion. la relation entre l'´erosion du sol par l'eau et les pr´ecipitations atmosph´eriques. Presses universitaires de France, Paris
Garzanti E, Andò S, Vezzoli G (2008) Settling-equivalence of detrital minerals and grain-size dependence of sediment composition. Earth Planet Sci Lett 273:138–151. https://doi.org/10.1016/j.epsl.2008.06.020
Garzanti E, Andò S, Vezzoli G (2009) Grain-size dependence of sediment composition and environmental bias in provenance studies. Earth Planet Sci Lett 277:422–432. https://doi.org/10.1016/j.epsl.2008.11.007
Guigue C, Tedetti M, HuyDang D, Mullot J, Garnier C, et al (2017) Remobilization of polycyclic aromatic hydrocarbons and organic matter in seawater during sediment resuspension experiments from a polluted coastal environment: insights from Toulon Bay (France). In: Environmental pollution, Vol. 229. Elsevier, pp 627–638. https://doi.org/10.1016/j.envpol.2017.06.090.hal-01635969.
Guzzella L, Depaolis A (1994) Polycyclic aromatic hydrocarbons in sediments of the Adriatic Sea. Mar Pollut Bull 28:59–165
Hassan M, Mirza ATM, Rahman T, Saha B, Kamal AKI (2015) Status of heavy metals in water and sediment of the Meghna River, Bangladesh. Am J Environ Sci 11:427–439
IARC (1987) Overall evaluations of carcinogenicity: an updating of IARC monographs Volumes 1 to 42. In: IARC monographs on the evaluation of carcinogenic risks to humans, vol. Supplement 7, Int Agency Res Cancer Lyon
Janaki-Raman D, Jonathan MP, Srinivasalu S, Armstrong-Altrin JS, Mohan SP, Ram-Mohan V (2007) Trace metal enrichments in core sediments in Muthupet mangroves, SE coast of India: application of acid leachable technique. Environ Pollut 145:245–257. https://doi.org/10.1016/j.envpol.2006.03.012
Jonathan MP, Ram Mohan V (2003) Heavy metals in sediments of the inner shelf off the Gulf of Mannar, South East Coast of India. Mar Pollut Bull 46:263–268. https://doi.org/10.1016/s0025-326x(02)00484-8
Kim GB, Maruya KA, Lee RF, Lee JH, Koh CH, Tanabe S (1999) Distribution and sources of polycyclic aromatic hydrocarbons in sediments from Kyeonggi Bay, Korea. Mar Pollut Bull 38:7–15. https://doi.org/10.1016/S0025-326X(99)80006-X
Kumar KSS, Nair SM, Salas PM, Peter KJP, Kumar CSR (2016) Aliphatic and polycyclic aromatic hydrocarbon contamination in surface sediment of the Chitrapuzha River, South-West India. Chem Ecol 32:117–135
Lebart L, Morineau A, Warwick KM (1984) Multivariate descriptive statistical analysis. Wiley, New York
Lee B-K, Vu VT (2010) Sources, distribution and toxicity of polyaromatic hydrocarbons (PAHs) in particulate matter, In: Air Pollut (London: IntechOpen), 99–122
Lei P, Pan K, Zhang H, Bi J (2019) Pollution and risk of PAHs in surface sediments from the tributaries and their relation to anthropogenic activities, in the main urban districts of Chongqing city, Southwest China. Bull Environ Contam Toxicol 103:28–33

Liu YP, Wang YH, Y, C, Xie B, Yang H, (2017) Sedimentary record of polycyclic aromatic hydrocarbons from the Shuanglong catchment Southwest China. J Chem. https://doi.org/10.1155/2017/4976574

Long ER, Mac Donald DD, Smith SL, Calde FD (1995) Incidence of adverse biological effects within ranges of chemical concentrations in marine and estuarine sediments. Environ Manag 19:81–97

MacDonald DD, Ingersoll CG, Berger TA (2000) Development and evaluation of consensus-based sediment quality guidelines for freshwater ecosystems. Arch Environ Contam Toxicol 39:20–31. https://doi.org/10.1007/s002440010075

Magdaleno F, Donadio C, Kondolf GM (2018) 30-year response to damming of a Mediterranean river in California, USA. Phys Geogr 39(3):197–215. https://doi.org/10.1080/02723646.2017.1361755

McLusky DS, Elliott M (2004) The estuarine ecosystem: ecology. Oxford University Press, Oxford, Threats and Management

Menon NN, Balchand AN, Menon NR (2000) Hydrobiology of the Cochin backwater system- a review. Hydrobiologia 430:149–183

Mill T, Mabey WR, Lan BY, Baraze A (1981) Photolysis of polycyclic aromatic hydrocarbons in water. Chemosphere 10:1281–1290

Mitra S, Ghosh S, Satpathy KK, Bhattacharya BD, Sarkar SK, Mishra P, Raja P (2017) Water quality assessment of the ecologically stressed Hooghly river Estuary, India: a multivariate approach. Mar Pollut Bull 126:592–599. https://doi.org/10.1016/j.marpolbul.2017.09.053

Mohtar ZA, Yahaya AS, Ahmad F (2015) Rainfall erosivity estimation for Northern and Southern peninsular Malaysia using Fournier indexes. Procedia Eng 125:179–184. https://doi.org/10.1016/j.proeng.2015.11.026

Mondal P, de Alcântara Mens R, Jonathan MP, Biswas JK, Murugan K, Sarkar SK (2018) Seasonal assessment of trace element contamination in intertidal sediments of the meso-macrotidal hooghly (Ganges) river estuary with a note on mercury speciation. Mar Pollut Bull 127:117–130. https://doi.org/10.1016/j.marpolbul.2017.11.041

Murphy PP, Bates TS, Curl JHC, Feely RA, Burger RS (1988) The transport and fate of particulate hydrocarbons in an urban fjord-like estuary. Estuar Coast Shelf Sci 27:461–482

Nisbet ICT, LaGoy PKI (1992) Toxic equivalency factors (TEFs) for polycyclic aromatic hydrocarbons (PAHs). Regul Toxicol Pharmacol 16:290–300

Norkko A, Thrush SF, Hewitt JE, Cummings VJ et al (2002) Smothering of estuarine sandflats by terrigenous clay: the role of wind-wave disturbance and bioturbation in site dependent macrofaunal recovery. Mar Ecol Prog Ser 234:23–41

Obini U, Okafor CO, Afuikwu JN (2013) Determination of level of polycyclic aromatic hydrocarbon in soil contaminated with spent motor engine oil in Abakaliki auto mechanic village. J Appl Sci Environ Manag 17:169–175

Parthasarathy B, Munot AA, Kothawale DR (1994) All-India monthly and seasonal rainfall series: 1871–1993. Theoret Appl Climatol. https://doi.org/10.1007/BF00867461

Rajaneesh KM, Mitbavkar S, Anil AC, Sawant SS (2015) Synechococcus as an in dicator of trophic status in the cochin backwaters, west coast of India. Ecol Indic 55:118–130

Rakshit D, Biswas SN, Sarkar SK, Bhattacharya BD, Godhantaraman N, Satpathy KK (2014) Seasonal variations in species composition, abundance, biomass and production rate of tintinnids (*Ciliata: Protozoa*) along the Hooghly (Ganges) river estuary, India: a multivariate approach. Environ Monit Assess 186:3063–3078. https://doi.org/10.1007/s10661-013-3601-9

Ravindra K, Wauters E, Van Grieken R (2008a) Variation in particulate PAHs levels and their relation with the transboundary movement of the air masses. Sci Total Environ 396:100–110

Ravindra K, Sokhi R, Van Grieken R (2008b) Atmospheric polycyclic aromatic hydrocarbons: source attribution, emission factors and regulation. Atmos Environ. https://doi.org/10.1016/j.atmosenv.2007.12.010

Ray R, Rixen T, Baum A, Malik A, Gleixner G, Jana TK (2015) Distribution, sources and biogeochemistry of organic matter in a mangrove dominated estuarine system (Indian Sundarbans) during the pre-monsoon. Estuar Coast Shelf Sci 167:404–413

Rogers KG, Goodbred SL, Mondal DR (2013) Monsoon sedimentation on the "abandoned" tide influenced Ganges-Brahmaputra Delta plain. Est Coast Shelf Sci 131:297–309. https://doi.org/10.1016/j.ecss.2013.07.014

Sadhuram Y, Sarma VV, Ramana Murthy TV, Rao BP (2005) Seasonal variability of physico–chemical characteristics of the Haldia channel of Hooghly estuary, India. J Earth Syst Sci 114:37–49. https://doi.org/10.1007/BF02702007

Sarkar SK, Binelli A, Chatterjee M, Bhattacharya BD, Parolini M, Riva C, Jonathan MP (2012) Distribution and ecosystem risk assessment of polycyclic aromatic hydrocarbons (PAHs) in core sediments of Sundarban mangrove wetland, India. Polycycl Aromat Comp 32:1–26. https://doi.org/10.1080/10406638.2011.633592

Sarkar SK (2016) Polycyclic aromatic hydrocarbons (PAHs) in sediment cores from Sundarban wetland. In: Sarkar, S.K. (Ed.), Marine organic micropollutants. Springer Int Publ Switzerland pp. 49–68. https://doi.org/10.1007/978-3-319-43301-1_4

Shetye SR (2011) Indian estuaries: dynamics, ecosystems, and threats. Natl Acad Sci Lett 34:229–237

Simpson CD, Mosi AA, Cullen WR, Reimer KJ (1996) Composition and distribution of polycyclic aromatic hydrocarbon contamination in surficial marine sediments from Kitimat Harbor, Canada. Sci Total Environ 181:265–278

Smith JN, Levy EM (1990) Geochronology of polycyclic aromatic hydrocarbon contamination in sediments of the Saguenay Fjord. Environ Sci Technol 24:874–879

Sunil Kumar R (1996) Distribution of organic carbon in the sediments of Cochin mangroves, south west coast of India. Indian J Mar Sci 25:274–276

Swartz RC (1999) Consensus sediment quality guidelines for PAH mixtures. Environ Toxicol Chem 18:780–787

Trifuoggi M, Ferrara L, Toscanesi M, Mondal P, Muthuswamy Ponniah J, Sarkar SK, Arienzo M (2022) Spatial distribution of trace elements in surface sediments of Hooghly (Ganges) river estuary in west Bengala, India. Environ Sci Pollut Res 29:6929–6942

US EPA (1977) Sampling and Analysis Procedures for Screening of Industrial Effluents for Priority Pollutants. U.S. Environmental Protection Agency, Environment Monitoring and Support laboratory, Cincinnati, US

US EPA (1993) Provisional Guidance for Quantitative Risk Assessment of Poly cyclic Aromatic Hydrocarbons. Environmental Criteria and Assessment Office. Office of Health and Environmental Assessment, Cnicinnati, US

US EPA (2008) Polycyclic Aromatic Hydrocarbons (PAHs)- EPA Fact Sheet. National Center for Environmental Assessment, Office of Research and Development, Washington, DC, US

Vineethaa G, Kripaa V, Karatib KK, Rehithac TV, Vishald CR, Vineethaa V, Manu M (2020) Impact of a catastrophic flood on the heavy metal pollution status and the concurrent responses of the bentho-pelagic community in a tropical monsoonal estuary. Mar Pollut Bull 155:111191

Wetz MS, Yoskowitz DW (2013) An "extreme" future for estuaries? Effects of extreme climatic events on estuarine water quality and ecology. Mar Pollut Bull 69:7–18

Wu B, Zhang R, Cheng SP, Ford T, Li AM, Zhang XX (2011) Risk assessment of polycyclic aromatic hydrocarbons in aquatic ecosystems. Ecotoxicology 20:1124–1130. https://doi.org/10.1007/s10646-011-0653-x

Yan B, Benedict L, Chaky DA, Bopp RF, Abrajano TA (2004) Levels and patterns of PAH distribution in sediments from New York/New Jersey Harbor complex. Northeast Geol Environ Sci 26:113–122

Zhang Y, Guo F, Meng W, Wang XQ (2009) Water quality assessment and source identification of Daliao river basin using multivariate statistical methods. Environ Monit Assess 152:105–121. https://doi.org/10.1007/s10661-008-0300-z

Zuloaga O, Prieto A, Ahmed K, Sarkar SK, Bhattacharya A, Chatterjee M, Bhattacharya BD, Satpathy KK (2013) Distribution of polycyclic aromatic hydrocarbons in recent sediments of Sundarban mangrove wetland of India and Bangladesh: a comparative approach. Environ Earth Sci 68:355–367. https://doi.org/10.1007/s12665-012-1743-7